International Journal of Progressive Sciences and Technologies (IJPSAT)
ISSN: 2509-0119.

http://ijpsat.ijsht-journals.org
Vol. 23 No. 2 November 2020, pp. 66-86

Induction Motor Windings Faults Detection Using Active and Reactive Power Based Model Reference Adaptive System Estimator

Jean Blaise TEGUIA [1,2], Georges Collince FOUOKENG [1*], and Godpromesse Kenne[2]

[1]Unite de Recherche de Matière Condensée, d'Electronique, d'Electrotechnique et de Traitement de signal (URMACET). Dept. of Physics, Faculty of Sciences, University of Dschang, P.O. Box 67, Dschang, Cameroon

[2]Research unit of Automation and Applied Computer (RU-AIA), Department of Electrical Engineering IUT-FV, University of Dschang, P.O. Box 134, Bandjoun, Cameroon

Abstract – The paper is concerned with detection of a stator and rotor winding faults in a squirrel-cage induction motor. The idea of the fault detection is based on a hypothesis that each of windings faults results in a sharp increase or decrease of internal parameters' values of the machine, therefore it can be treated as a suitable fault symptom. Resistances of the stator and rotor windings seem to be adequate quantities due to their direct relationship with the machine windings. An observation and analysis of the parameters' changes in a real- time domain enables to an incipient detection of the fault. It is evident that internal parameters of the machine can't be measured directly during operation on the drive system thus the only way is an estimation by specialized algorithms. In the paper two estimators based on active (P) and reactive (Q) power based Model Reference Adaptive System (PQ-MRAS) estimators were utilized to achieve this goal. The estimator employs the active (P) and reactive (Q) power of the machine which is calculated by the only measurable signals, such as stator voltage and current. Two simple algorithms for faults detection are proposed as well. Detailed description of fault detection systems is included in the paper. Proposed systems were tested on computer simulations performed by MATLAB/Simulink software.

Keywords – Induction Motor, Stator Fault, Rotor Fault, Faults Detection, Parameter Estimator, MRAS, Active Power, Reactive Power.

I. Introduction

Electric drives with induction motors (IM) are basic components in various systems, such as electric and hybrid cars, trams, trains, metro, power plants and industrial machines [1]. During operation of any electrical drive, damage of its components can be occurred including sensors (electrical or mechanical), power electronics devices and the machine [2], [3]. Internal faults of the machine can be divided into mechanical and electrical [2], [4]. According to the literature up to 40% of faults belong to the stator windings and about 10% to the rotor winding.

Other faults are related to the bearing and another machine's components [5], [3]. Stator windings damages are related to an insulation degradation, what causes interturn short-circuit (ITSC) within a coil, while broken rotor bars and end-rings are electrical faults in the cage of the IM [4]. Motor's winding faults have a negative impact on the operation of the drive, and they should be detected as soon as possible, to avoid further degradation of the machine and enable a safety stop of the drive [4], [6], [5], [3].

Several diagnostics techniques related to stator and rotor windings faults have been developed.

One of the most popular method is the signal- based (SB) diagnostic procedure [4], [6]. This technique consists of an analysis of measured signals such as: current, voltage, electromagnetic flux, power, mechanical vibration, angular speed and temperature [7], [3]. The analysis is performed on time, frequency or time-frequency domains to extract specific symptoms which are related to the faults [4]. These methods often utilize signal analysis techniques, which are based on the Fast Fourier Transform (FFT), Short Time Fourier Transform (STFT), Wavelet Transform (WT), Hilbert Transform (HT) [6], [3] etc. To improve an effectiveness of the faults diagnosis, these methods are often supported by solutions based on artificial intelligence (AI) (artificial neural networks (ANN), fuzzy logic (FL)) [6], [3], [8].

Nowadays, it has become a standard, that IM's work in closed-loop control systems what enable to precise regulation of IM's electromagnetic torque or the angular speed [1], [7]. However, closed-loop control systems (including vector control algorithms) can compensate effects of windings faults, what complicates the extraction of the faults symptoms from measured signals (f. ex. Stator currents) [9], [10]. Several signal-based diagnostics methods for closed-loop control systems are developed and presented in papers [10], [11], [12], [13], [14], [15], [16].

Another approach to damages detection is the model-based (MB) fault diagnosis technique which in general relies on a mathematical model of the machine [4], [17], [18], [3]. One of these methods is based on hypothesis, that winding faults symptoms can be observed as changes (a sharp decrease/increase, oscillations) of values of the IM parameters [19], [20], [17]. This method requires an identification of the IM parameters during its operation. Several identification algorithms have been utilized in a context to the IM's stator or rotor windings faults diagnosis. They have based on: last square error minimization [20], Kalman Filter [22], [22], [23], [24], [25], [26], [27], nonlinear programming [21], state observers [23], [28], [29], Moving Horizon Estimation, [30], [31], genetic algorithm [31], Sparse grid optimization [32], trust- region and Broyden-Fletcher-Goldfard-Shano (TR- BFGS) technique [30], and Sliding Mode Observer [34].

Despite, that many identification algorithms have been tested in a context to the IM's fault detection, not all existing approaches have been taken into consideration. One of them are estimators based on Model Reference Adaptive System (MRAS), which are often utilized in the IM drives to calculate state variables and parameters of the machine [35], [36], [37]. The major drawback of the proposed approach is the fact that both (adjustable and reference) models are directly dependent on the estimated parameters. The PQ-MRAS estimator which enables the estimation of both resistances simultaneously. It is based on the active and reactive powers of the induction motor. The main benefits of proposed estimator are that reference models are calculated using only measurable signals, such as current, voltage and rotor speed [45].

Therefore, in this paper a two estimators based on active (P) and reactive (Q) power based Model Reference Adaptive System (PQ-MRAS) estimators are used to the IM's parameters identification in order to rotor or stator faults detection. Two estimators are utilized: first one [46], [47] is used to the rotor resistance estimation while second [47], [48] is used to the stator resistance estimation. Estimated parameters are utilized in faults detection algorithms, which are based on two simple assumptions [39], [41]:

• first – connected with rotor windings faults – rupture of a rotor's bar(s) results in a sharp increase of the estimated rotor resistance;

•second – connected with stator windings faults – ITSC results in a sharp decrease of the estimated stator resistance.

Due to the fact, that values of both resistances are strongly dependent on windings temperature (heating or cooling process), proposed algorithms were tested also for this phenomenon.

Studies were performed in the closed-loop control system based on Direct Field Oriented Control (DFOC) structure.

In the paper results of computer simulation studies are shown which were carried out by MATLAB/Simulink software.

The article is composed of several sections. In Section 2 a Mathematical Model of the induction motor for the rotor and the stator windings faults. A detailed description of estimators of induction motor parameters based on the PQ-MRAS estimator is presented in section 3 [46]. Section 4 includes the explanation of the vector control structure for the induction motor, while Section 5 presents the algorithms for the induction motors 's windings faults detection. Section 6 discusses the results of simulation tests.

II. Mathematical Model Of The Induction Motor For The Rotor And The Stator Windings Faults

During computer simulations, a mathematical model of the IM with possibility to tests the stator and rotor windings faults are necessary. In the paper two types of mathematical models were used which are described in the stationary reference frame (α-β). The first model to the stator faults analysis, the second one for the rotor faults analysis.

In this chapter the control structure is also presented.

2.1. Model of the induction motor for the stator windings faults

To the ITSC simulation, a model proposed in [30] was used.

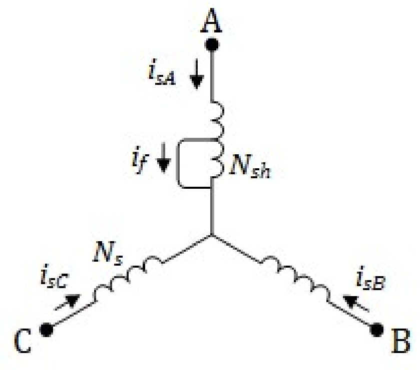

Fig.1. ITSC in a phase A of the IM

It can be assumed [29], that the total number of turns in each phase is N_S and amount of s horted turns in N_{sh}. Relative number of shorted turns is $\eta f = N_{sh}/N_S$. Fig. 1 illustrates the scheme of the IM's stator windings with a short circuit in the phase A. The short circuit is characterized by the short-circuit current i_f and its resistance r_f. The inductance of the short circuit is assumed to be negligible and is not taken into account.

Flux ψf is induced in the short circuit, therefore the voltage equation of the short circuit in phase A can be described as:

$$T_N \frac{d\psi_f}{dt} = R_f i_f - \eta_{fA} R_s + \left(i_{sA} - i_f\right), \quad (1)$$

The voltage equations for the remaining phases can be derived respectively.

Equation (1) can be transformed to α-β stationary reference frame in the following way:

$$T_N \frac{d\psi_f}{dt} = R_f i_f - R_s\left(\mu_\alpha i_{s\alpha} + \mu_\beta i_{s\beta}\right) + \left|\mu_{\alpha\beta}\right| R_s i_f, \quad (2)$$

where: R_s – stator windings resistance, R_f – shorted circuit resistance, i_f – shorted circuit current, i_s – stator current vector, $T_N = 1/\left(2\pi f_{sN}\right)$, $\left|\mu_{\alpha\beta}\right|$ is a modulous of the vector, $\mu_{\alpha\beta} = \left[\mu_\alpha \quad \mu_\beta\right]^T$ which indicates the relative value and the direction (phase) of the short circuit. Depending on which phase is faulty, it can take the following forms: wich indicate the fraction of the shorted turns and a phase of the short corcuit respectively.

$$\mu_{\alpha\beta|A} = \eta_{fA}\left[0 \quad 1\right]^T, \quad (3a)$$

$$\mu_{\alpha\beta|B} = \eta_{fB}\left[-\frac{1}{2} \quad \frac{\sqrt{3}}{2}\right]^T, \quad (3b)$$

$$\mu_{\alpha\beta|C} = \eta_{fC}\left[-\frac{1}{2} \quad -\frac{\sqrt{3}}{2}\right]^T, \quad (3c)$$

where $\eta_{fA}, \eta_{fB}, \eta_{fC}$, relative amount of shorted turns for each phase. The current in the short circuit can be obtain by the equation :

$$i_f = \frac{\psi_f - \left(\mu_\alpha \psi_{s\alpha} + \mu_\beta \psi_{s\beta}\right)}{\left(\frac{2}{3}\left|\mu_{\alpha\beta}\right|^2 - \left|\mu_{\alpha\beta}\right|\right) L_{\sigma s}}, \quad (4)$$

Where $L_{\sigma s}$ – stator leakage inductance. The stator flux vector components $\psi_{s\alpha}$, $\psi_{s\beta}$ can be calculated from modified differential equations of the stator windings (5a , 5b). Thus the stator and rotor voltage equations are:

$$T_N \frac{d\psi_s}{dt} = u_s - R_s\left(i_s - \frac{2}{3}\mu_{\alpha\beta} i_f\right), \quad (5a)$$

$$T_N \frac{d\psi_{s\beta}}{dt} = u_{s\beta} - R_s\left(i_{s\beta} - \frac{2}{3}\mu_\beta i_f\right), \quad (5b)$$

$$T_N \frac{d\psi_{r\alpha}}{dt} = -R_r i_{r\alpha} - \omega_m \psi_{r\beta}, \quad (5c)$$

$$T_N \frac{d\psi_{r\beta}}{dt} = -R_r i_{r\beta} + \omega_m \psi_{r\alpha}, \quad (5d)$$

where : $\mathbf{u_S}$ – stator voltage vector, $\mathbf{i_S}$ – stator windings resistance, $\boldsymbol{\psi}_\mathbf{r}$ – stator flux vector, R_r – rotor windings resistance, ω_m – angular rotor speed.

The flux-current equations of the stator and rotor circuits become:

$$i_{s\alpha} = \frac{L_r}{w}\psi_{s\alpha} - \frac{L_m}{w}\psi_{r\alpha} + \frac{2}{3}\mu_\alpha i_f, \quad (6a) \;;$$

$$i_{s\beta} = \frac{L_r}{w}\psi_{s\beta} - \frac{L_m}{w}\psi_{r\beta} + \frac{2}{3}\mu_\beta i_f, \quad (6b)$$

$$i_{r\alpha} = \frac{L_s}{w}\psi_{r\alpha} - \frac{L_m}{w}\psi_{s\alpha}, \quad (6c) \;;$$

$$i_{r\beta} = \frac{L_s}{w}\psi_{r\beta} - \frac{L_m}{w}\psi_{s\beta}, \qquad (6d)$$

where: $L_r = L_m + L_{r\sigma}$, $L_s = L_m + L_{s\sigma}$. L_r, L_s - rotor and stator inductance, $L_{r\sigma}$, $L_{s\sigma}$ - rotor and stator leakage inductance, L_m - main inductance, $w = L_s L_r - L_m^2$. Electromagnetic torque T_E and the equation of motion are:

$$T_E = \psi_{s\alpha}\left(i_{s\beta} - \frac{2}{3}\mu_\beta i_f\right) - \psi_{s\beta}\left(i_{s\alpha} - \frac{2}{3}\mu_\alpha i_f\right), \qquad (7)$$

;

$$\frac{d\omega_m}{dt} = \frac{1}{J}\left(T_E - T_L\right), \qquad (8)$$

where: T_E – electromagnetic torque, T_L – load torque, L_s, L_r, L_m – stator, rotor, mutual inductance, respectively, J—inertia of the shaft.

2.2. Model of the induction motor for the rotor windings faults

To the rotor bars damage simulation, the model proposed in [41] was used. This model assumes that a rupture of each of the rotor's bar results in an increase of the rotor resistance value. Rotor resistance components in *α-β* coordinates system are obtained by:

$$R_{r\alpha} = \frac{N_b R_{rN}}{2\sum_{k=1}^{N_b} G_w(k)\sin^2\left(\theta + \frac{2\pi k}{N_b}\right)}, \qquad (9)$$

$$R_{r\alpha} = \frac{N_b R_{rN}}{2\sum_{k=1}^{N_b} G_w(k)\sin^2\left(\theta + \frac{2\pi k}{N_b} - \frac{\pi}{2}\right)}, \qquad (10)$$

where: N_b –number of rotor bars, θ – angle of rotor position, G_W – vector of rotor bars conductance, where each element corresponds to rotor bar condition (if $G_w(k) = 0$ – faulted, $G_w(k) = 1$ - healthy).

Rotor resistance components calculated by (9-10) are used in the rotor voltage equation (5a-5b) instead of the constant R_r parameter. When N_b = 0 rotor resistance components are equal to the nominal value of this quantity. During rotor bars faults obtained rotor resistance components oscillate, what results in stator currents modulation.

III. Estimators Of Induction Motor Parameters Based On The PQ MRAS Estimator

The proposed estimator consists of two subsystems:

- P-MRAS—based on the active power (P) of the machine; it is used to calculate the stator resistance.
- Q-MRAS—based on the reactive power (Q) of the machine; it is used to calculate the rotor resistance.

Each subsystem has its own independent adaptation mechanism based on a PI (Proportional–Integral) controller. The common part of P and Q-MRAS is the rotor flux estimator.

A reference model of the P-MRAS is given by:

$$P^{ref} = \mathrm{Re}\{u_s \cdot i_s *\} = u_{s\alpha} \cdot i_{s\alpha} + u_{s\beta} \cdot i_{s\beta}, \qquad (11)$$

where $\mathbf{u_s} = u_{s\alpha} + ju_{s\beta}$ — stator voltage vector, $\mathbf{i_s} = i_{s\alpha} + ji_{s\beta}$ — stator current vector, $\mathbf{i_r} = i_{r\alpha} + ji_{r\beta}$ — rotor current vector, $\boldsymbol{\psi_r} = \psi_{r\alpha} + j\psi_{r\beta}$ — rotor electromagnetic flux vector, $\boldsymbol{\psi_s} = \psi_{s\alpha} + j\psi_{s\beta}$—stator electromagnetic flux vector, ω_m —rotational shaft speed, T_E — electromagnetic torque, T_L—load torque. R_s, R_r—stator, rotor resistances respectively; L_s, L_r, L_m—stator, rotor, magnetizing inductances, respectively; p_b—number of pole pairs, J—inertia of the shaft, $w = L_s L_r - L_m^2$, $\sigma = 1 - \frac{L_m^2}{L_s L_r}$.

In an adjustable model, estimated stator voltage is used instead of the measured one. The estimated stator voltage vector can be expressed as:

$$u_s^{est} = R_s i_s + \frac{L_m}{L_r}\frac{d\psi_r^{est}}{dt} + \sigma L_s \frac{di_s}{dt}, \qquad (12)$$

Finally, the formula of P-MRAS adjustable model is :

$$P^{adj} = \mathrm{Re}\{u_s^{est} \cdot i_s *\} = R_s^{est}\left(i_{s\alpha}^2 + i_{s\beta}^2\right) + \sigma L_s\left(i_{s\alpha}\frac{di_{s\alpha}}{dt} + i_{s\beta}\frac{di_{s\beta}}{dt}\right) + \frac{L_m}{L_r}\left(i_{s\alpha}\frac{d\psi_{r\alpha}^{est}}{dt} + i_{s\beta}\frac{d\psi_{r\beta}^{est}}{dt}\right), \qquad (13)$$

It can be observed that the value of active power, calculated by the adjustable model, directly depends on stator resistance. Therefore, the role of stator resistance adaptation mechanism is the minimization of the error between the two models:

$$\varepsilon_P = P^{ref} - P^{adj}, \quad (14);$$

$$R_s^{est} = K_{PRs}\varepsilon_P + K_{IRs}\int \varepsilon_P dt, \quad (15)$$

where K_{PRs}, K_{IRs}— coefficients of the proportional and integral terms, respectively.

Rotor flux components in (16) are derived from the current model estimator [49]:

$$\psi_r^{est} = \int\left(\frac{R_r}{L_r}\left(L_m i_s - \psi_r^{est}\right) + jp_b\omega_m\psi_r^{est}\right)\mathrm{dt}, \quad (16)$$

The reference model of the Q-MRAS is given by:

$$Q^{ref} = \mathrm{Im}\{u_s \cdot i_s *\} = u_{s\beta}\cdot i_{s\alpha} - u_{s\alpha}\cdot i_{s\beta}, \quad (17)$$

whereas the adjustable model of this subsystem uses the estimated value of the stator voltage (12):

$$Q^{adj} = \mathrm{Im}\{u_s^{est}\cdot i_s *\} = \sigma L_s\left(i_{s\alpha}\frac{di_{s\alpha}}{dt} - i_{s\beta}\frac{di_{s\alpha}}{dt}\right) + \frac{L_m}{L_r}\left(i_{s\alpha}\frac{d\psi_{r\beta}^{est}}{dt} - i_{s\beta}\frac{d\psi_{r\alpha}^{est}}{dt}\right), \quad (18)$$

In this model the dependence on the rotor resistance is implicit. It consists of the rotor flux components which are calculated by the current model (16) which directly depends on the value of this parameter. The rotor resistance adaptation mechanism minimizes the error between the reference and adjustable models :

$$\varepsilon_Q = \left|Q^{ref}\right| - \left|Q^{adj}\right|, \quad (19);$$

$$R_r^{est} = K_{PRr}\varepsilon_Q + K_{IRr}\int \varepsilon_Q dt, \quad (20)$$

where K_{PRr}, K_{IRr}—coefficients of the proportional and integral terms, respectively. The sign of the reactive power is changed due to the shaft rotational speed reversals, therefore in the adaptation mechanism the absolute values of Q^{ref} and Q^{adj} are used. In Figure 2 a block diagram of the PQ-MRAS estimator is shown.

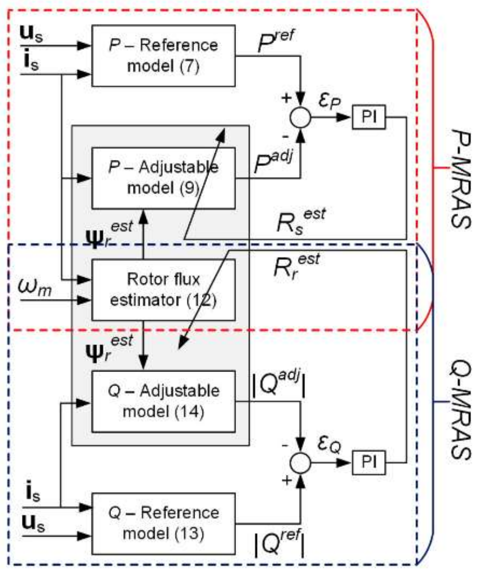

Figure 2. Scheme of the PQ-MRAS estimator.

IV. Description Of The Vector Control Structure For Induction Motor

Direct Field Oriented Control (DFOC) structure has become a commonly-known and popular control method which allows to control the speed of the induction motor drive precisely and similarly to the separately-excited DC motor. A block diagram of the control structure is shown in Figure 3.

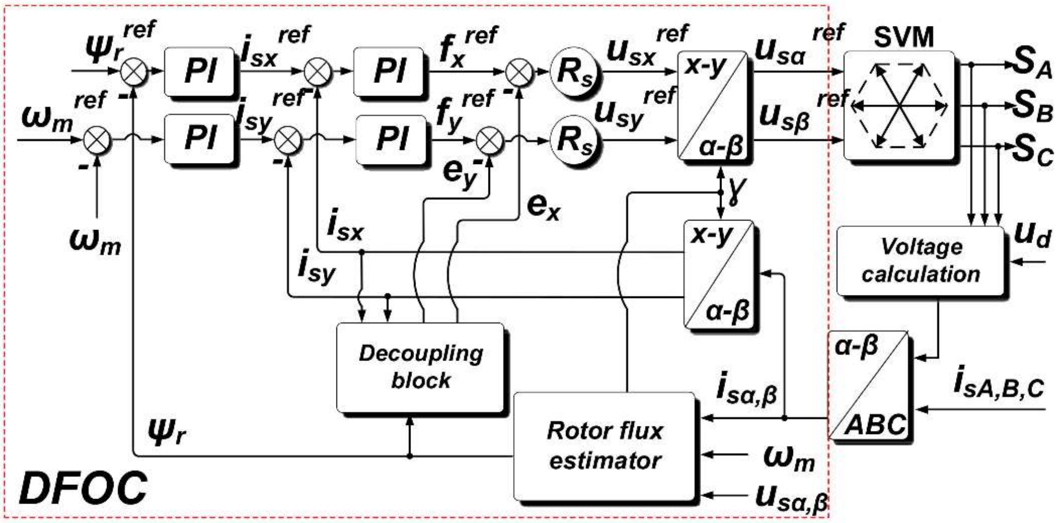

Figure 3. Scheme of the DFOC system.

The main part of the control structure are the four controllers (PI-type in this paper): two outer ones which control the speed and amplitude of the rotor flux (weakened when the speed exceeds the nominal value), and two inner ones to control the components of the stator current vector. The reference voltage vector components are the inputs of the Space Vector Modulation block, which ensures that the real voltages are the same as the desired ones, and defines the transistor on/off signals S_A, S_B and S_C. These three signals, and the DC voltage value *ud* , are then used to estimate the voltage vector components, if they are necessary in the operation of a flux estimator.

The outputs of the PI current controllers could be the reference voltage vector components in synchronous *x-y* frame directly, however, it is known that the control paths are both coupled (21a), (21b). The stator and rotor voltage equations in the synchronous reference frame, rotating with the rotor flux vector velocity $\omega\psi r$ are as follows:

$$u_{sx} = R_s i_{sx} + \sigma L_s T_N \frac{di_{sx}}{dt} + \frac{L_m}{L_r} T_N \frac{d\psi_r}{dt} - L_s \sigma \omega_{\psi r} \mathrm{i}_{sy}, \qquad (21a)$$

$$u_{sy} = R_s i_{sy} + \sigma L_s T_N \frac{di_{sy}}{dt} + \frac{L_m}{L_r} \omega_{\psi r} \psi_r + L_s \sigma \omega_{\psi r} \mathrm{i}_{sx}, \qquad (21b)$$

$$u_{rx} = 0 = L_m i_{sx} - \psi_r + \frac{L_r}{R_r} T_N \frac{d\psi_r}{dt} \qquad (21c) \; ; \qquad u_{ry} = 0 = \frac{R_r L_m}{L_r} i_{sy} - \left(\omega_{\psi r} - \omega_m\right)\psi_r \qquad (21d)$$

where : $\sigma = 1 - \frac{L_m{}^2}{L_s L_r}$

Due to the coupling in the control paths, the decoupling block is applied, and the idea of the decoupling is shown in Fig. 4. For the purpose of the figure, it is assumed that the voltage modulator is ideal, and the reference voltage is equal to the real one, without any delay. If the decoupling signal *ex* is estimated correctly, the control path reduction (-*ex*, +*ex*) causes the strict control of the *isx* component by the output of the *Risx* controller, and therefore this component is independent on the remaining variables (as in (21a)). The second control path is decoupled respectively.

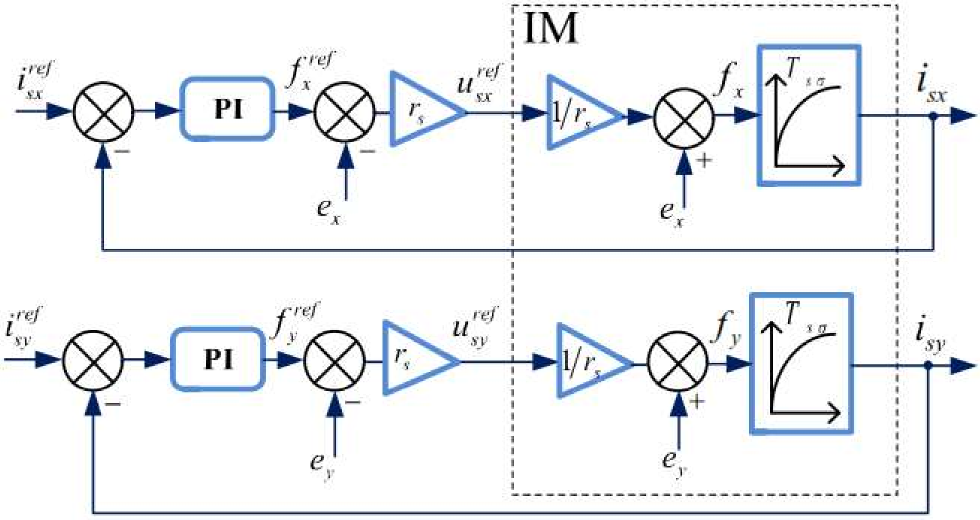

Fig. 4.The idea of the control paths decoupling for induction motor field oriented control

The decoupling of the control paths can be presented in terms of the following expressions:

$$f_x = \frac{1}{R_s} u_{sx} + e_s, \qquad (22a)$$

where $f_x = i_{sx} + T_{s\sigma} \frac{di_{sx}}{dt}$, $e_x = -\frac{L_m}{R_s L_r} T_N \frac{d\psi_r}{dt} + \frac{L_s \sigma}{R_s} \omega_{\psi r} \mathrm{i}_{sy}$, $T_{s\sigma} = \frac{\sigma T_N L_s}{R_s}$

$$f_y = \frac{1}{R_s} u_{sy} + e_y, \qquad (22b)$$

where $f_y = i_{sy} + T_{s\sigma} \frac{di_{sy}}{dt}$, $e_y = -\frac{L_m}{R_s L_r} \omega_{\psi r} \psi_r - \frac{L_s \sigma}{R_s} \omega_{\psi r} \mathrm{i}_{sx}$,

The decoupling block (Fig. 3) calculates the decoupling signals using the expressions from (22). The synchronous velocity $\omega\psi r$ can be calculated, after some simple transformation, from (21d). As it will be shown in the next section, the decoupling signals *ex*, *ey*, and the control signals f_x^{ref}, f_y^{ref} carry very useful diagnostic information. These control variables will be utilized by the proposed diagnostic method of the short-circuit turns of the IM stator winding.

Voltage vector components were calculated using control signals and measured DC bus voltage from a Voltage Source Inverter (VSI):

$$u_{s\alpha} = \frac{2}{3} u_d \left(S_A - \frac{1}{2} \left(S_B + S_C \right) \right), \quad (23)$$

$$u_{s\beta} = \frac{\sqrt{3}}{3} u_d \left(S_B + S_C \right), \quad (24)$$

The PQ-MRAS estimator can operate in two modes (Figure 4):

•Open-loop mode—independently of the control structure;

• Closed-loop mode—coupled with the control structure; the estimated parameters are injected to the control structure (flux estimator).

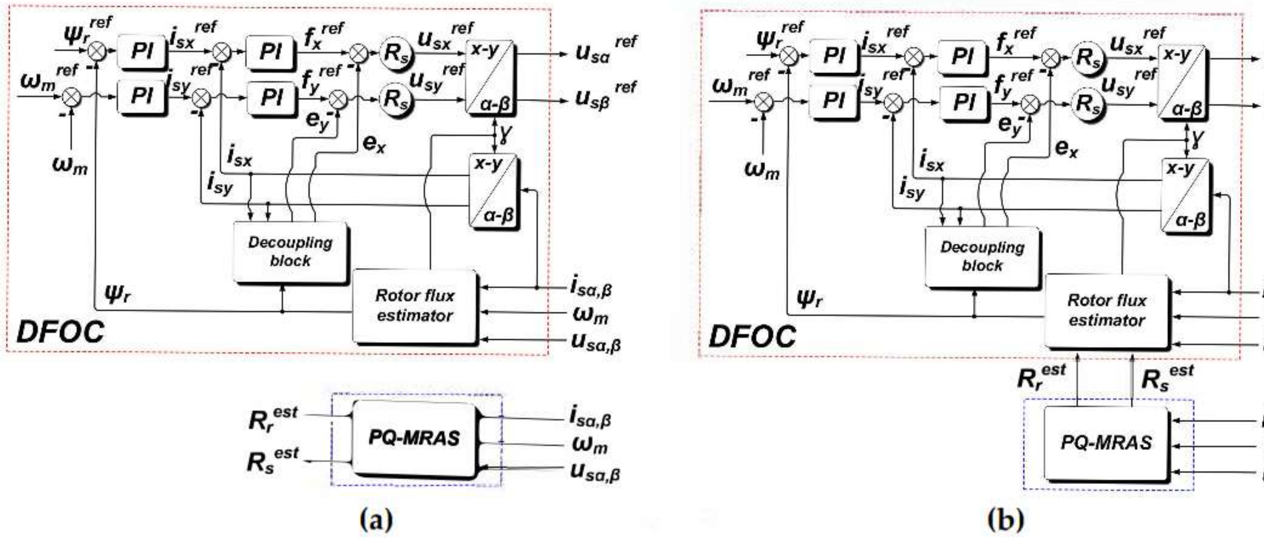

Figure 4. Operation of the PQ-MRAS estimator: (a) open-loop mode, (b) closed-loop mode.

V. ALGORITHMS FOR THE INDUCTION MOTORS 'S WINDINGS FAULTS DETECTION

Two winding faults detection algorithms are discussed in the paper. The algorithms cooperate with estimators of windings resistance. A general idea of a detection system is illustrated in Fig. 5. The system is strictly related to the model-based fault detection approach [17], [18].

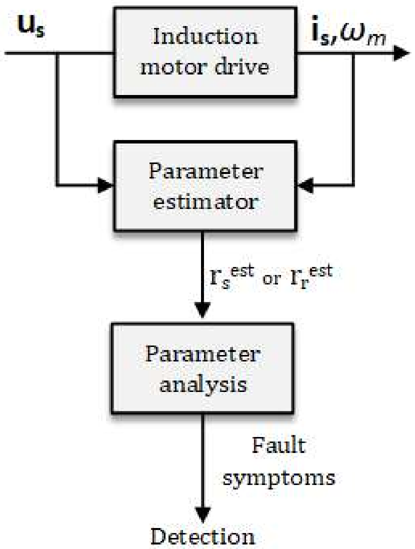

Fig. 5. The main idea of the diagnostic system for IM drive

In the further part of this section a detailed descriptions of detection procedures are presented.

5.1. The rotor fault detection algorithm

The rotor winding faults detection algorithm assumes that ruptures of the rotor bar(s) results in a sharp increase of the estimated rotor resistance. According to the assumption, a simple detection method is proposed which uses a derivative of the estimated rotor resistance:

$$\text{If} \quad \left| \frac{d}{dt} R_r^{est} \right| \geq \varepsilon_{Rr} \quad \text{then 1 else 0,} \qquad (28)$$

where: ε_{Rr} - threshold of a rotor windings fault detection.

When the modulus of the derivative is greater or equal to the fixed threshold the detector sends a logical 1 which indicates on a bar damage.

5.2. The stator fault detection algorithm

The stator winding faults detection algorithm is analogous to the previous one. It assumes, that ITSC results in a sharp decrease of the estimated stator resistance. Based on this hypothesis, the detection method is proposed, which uses a derivative of the estimated stator resistance:

$$\text{If} \quad \left| \frac{d}{dt} R_s^{est} \right| \geq \varepsilon_{Rs} \quad \text{then 1 else 0,} \qquad (29)$$

where: ε_{Rs} - threshold of a stator windings fault detection.

If the modulus of the derivative is equal of greater to the threshold the detector sends the logical 1, which indicates on occurring of ITSC.

VI. SIMULATION RESULTS

The rated data of the tested induction motor are summarized in Table A1. During the simulation and experimental tests, the values of adaptation mechanism coefficients were the same (Table A2). State variables from the drive, such as: rotational speed, electromagnetic torque, rotor flux and stator current are presented along with internal signals from the PQ-MRAS estimator: active and reactive powers, estimated stator and rotor resistances. Each of the signals and state variables is normalized to its nominal value.

Simulation tests were performed using Matlab-Simulink software using Euler method with sampling time 1e-6 s.

During the simulations, the estimator was tested for the open-loop as well as closed-loop operation modes. In a simulation model, effects such as signal offsets, measurements noise and inverter nonlinearity were not taken into consideration.

Table A1. IM Data.

Symbol	Rated Data	Value	Unit
P_N	Power	1.1	kW
U_N	Stator voltage	400	V
I_N	Stator current	2.8	A
n_N	Mechanical speed	1360	rpm
tN	Torque	7.7	Nm
R_s	Stator resistance	5.9	Ω
R_r	Rotor resistance	4.5	Ω
L_s	Stator inductance	451.0	mH
L_r	Rotor inductance	451.0	mH
L_m	Magnetizing inductance	424.4	mH
J	Inertia	0.0143	$kg\cdot m^2$
p_b	Pole pairs	2	-
η	Efficiency	0.79	-

Table A2. Coefficients of PI controllers in adaptation mechanism.

Symbol	Value
K_{PRs}	10
K_{IRs}	20
K_{PRr}	2
K_{IRr}	0.25

6.1. Operation of the PQ-MRAS in Open-Loop Mode

The main goal of the first test was to check the general performance of the PQ-MRAS. The results are presented in Figures 5 and 6. It can be observed that both estimated parameters tracked real values with high accuracy.

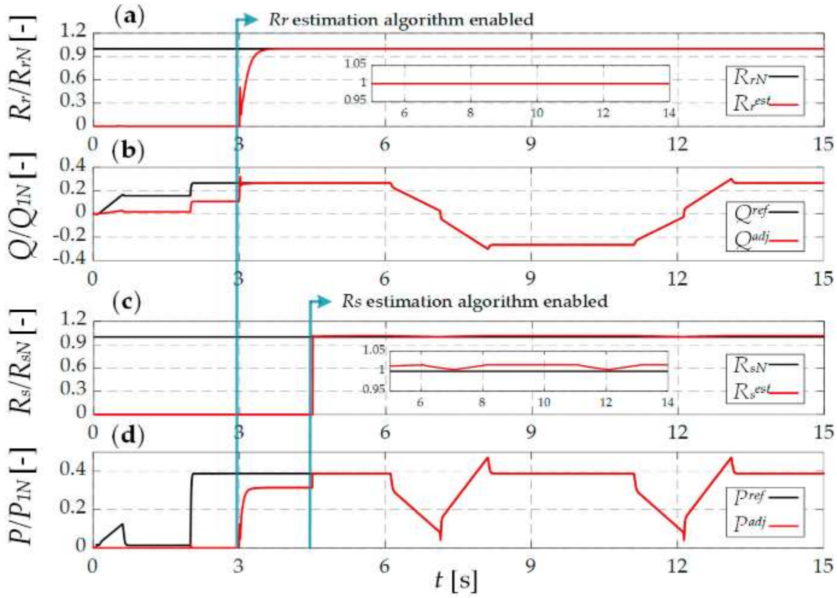

Figure 5. Operation of the PQ-MRAS estimator: (a) estimated rotor resistance, (b) reference and estimated reactive power, (c) estimated stator resistance, (d) reference and estimated active power; (simulation results), (ωm ref = ±0.5 ωmN, tL = ±0.75 tN, Rr = RrN , Rs = RsN).

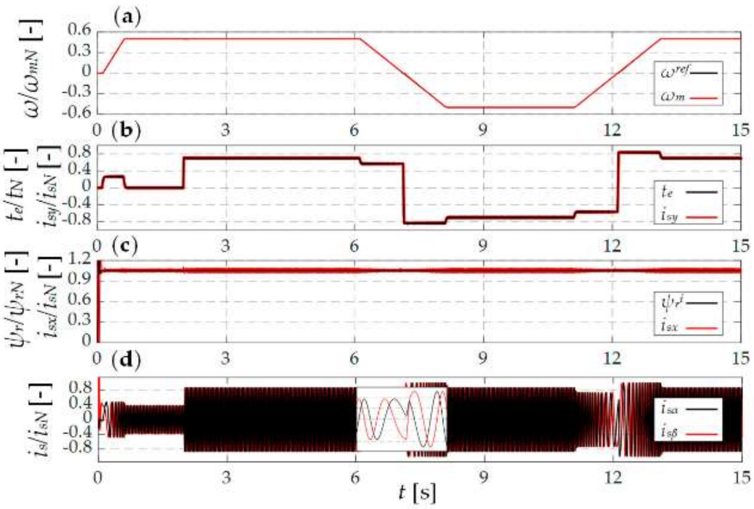

Figure 6. State variables of the drive: (a) reference and simulated rotational speed, (b) electromagnetic torque and stator current component isy , (c) estimated rotor flux vector module and stator current component isx , (d) stator current components isα,β ; (simulation results), (ωm ref = ±0.5 ωmN, tL = ±0.75tN, Rr = RrN , Rs=RsN).

Even during speed reversal variations the estimated parameters were negligible (maximum estimation error for stator resistance increased to 2%). During the second test, the robustness of the estimator to load torque variations was considered. The obtained results (Figures 7 and 8) show that both parameters were calculated with high accuracy even for load variations.

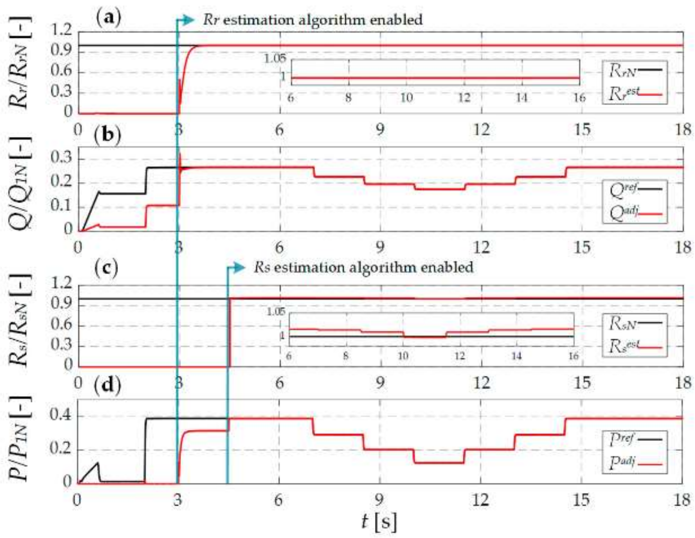

Figure 7. Operation of the PQ-MRAS estimator: (a) estimated rotor resistance, (b) reference and estimated reactive power, (c) estimated stator resistance, (d) reference and estimated active power; (simulation results), (ωm ref = 0.5 ωmN, tL = var, Rr = RrN , Rs = RsN).

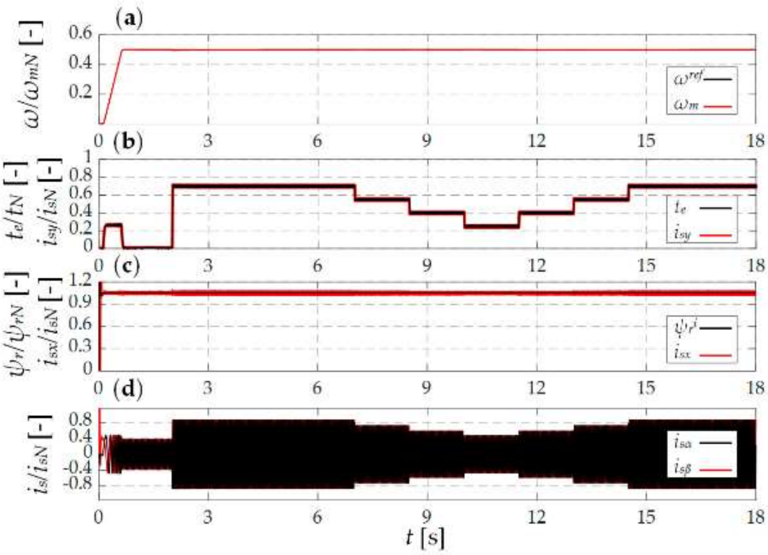

Figure 8. State variables of the drive: (a) reference and simulated rotational speed, (b) electromagnetic torque and stator current component isy , (c) estimated rotor flux vector module and stator current component isx , (d) stator current components isα,β ; (simulation results), (ωm ref = 0.5 ωmN, tL = var, Rr = RrN , Rs = RsN).

The aim of the next analysis was to check how the values of adaptation mechanism coefficients impact the estimator performance. Figure 9 shows a comparison of estimator signals for different sets of coefficients: nominal values (Appendix B), nominal values multiplied by 5 and nominal values divided by 5. The coefficient values have a major impact on the dynamics of the estimator, nevertheless it operated in a stable manner.

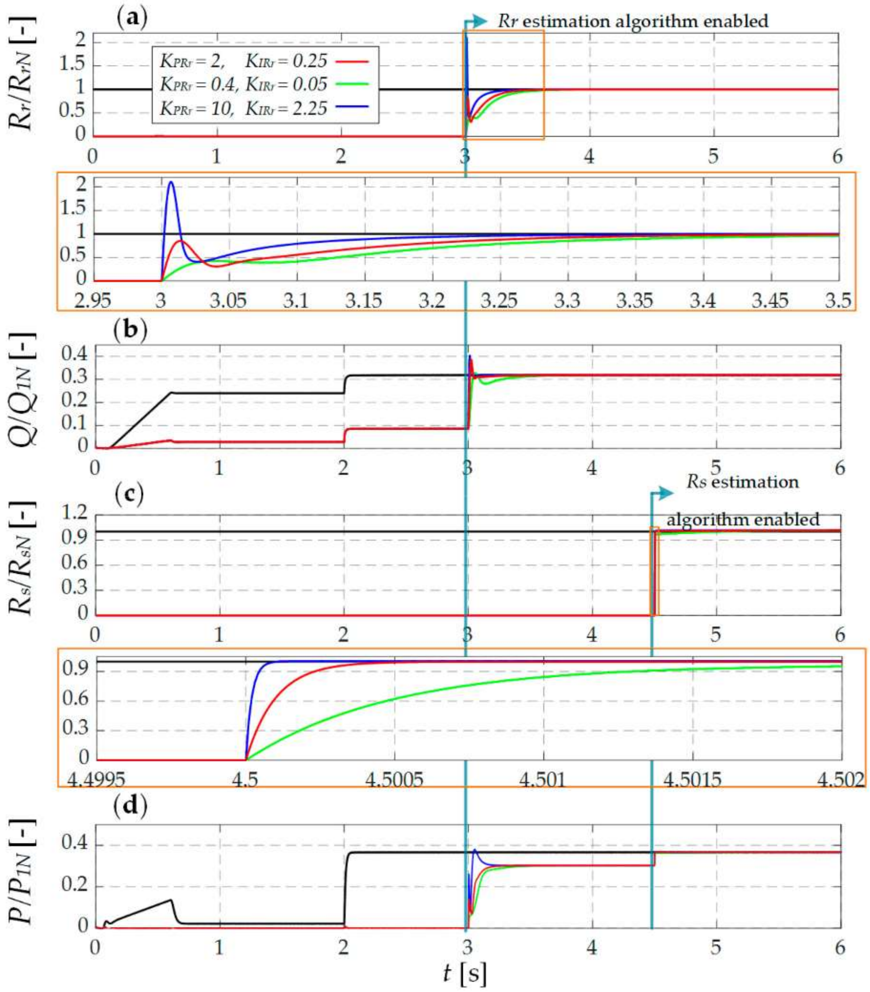

Figure 9. Operation of the PQ-MRAS estimator for different values of parameters in adaptation mechanisms: (a) estimated rotor resistance, (b) reference and estimated reactive power, (c) estimated stator resistance, (d) reference and estimated active power; (simulation results), (ωm ref = 0.5 ωmN, tL = 0.75 tN, Rr = RrN , Rs = RsN).

During the next test, it was assumed that both resistances increased up to 150% of their nominal values, which was related to the changes of machine windings temperatures. It can be seen that both resistances were estimated correctly (Figure 10). Due to rotor resistance variations, the estimation error of the rotor flux can be observed (Figure 11), because the current model is directly influenced by this parameter (17). The inaccurate calculation of the rotor flux vector results in the coupling of flux and torque control paths, which consequently results in the deterioration of drive performance.

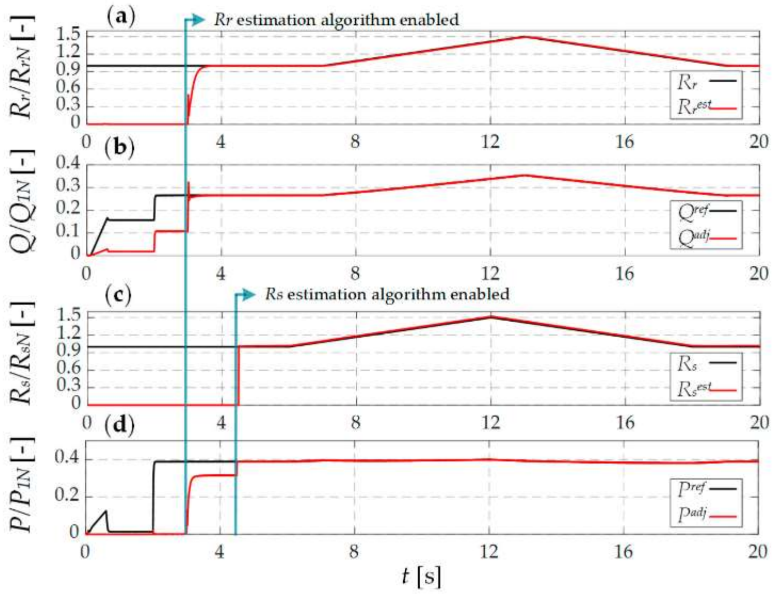

Figure 10. Operation of the PQ-MRAS estimator: (a) estimated rotor resistance, (b) reference and estimated reactive power, (c) estimated stator resistance, (d) reference and estimated active power; (simulation results), (ωm ref = 0.5 ωmN, tL = 0.75 tN, Rr = var, Rs = var).

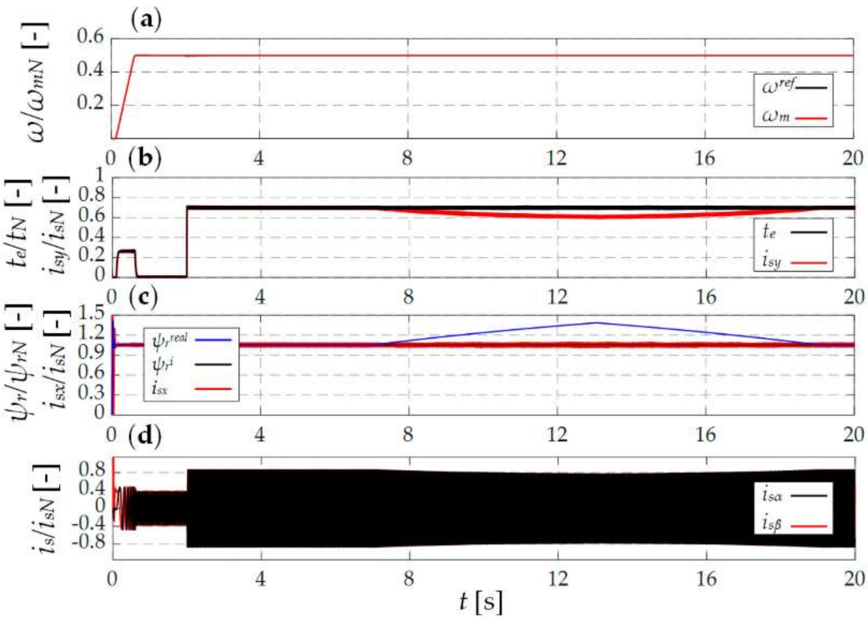

Figure 11. State variables of the drive: (a) reference and measured rotational speed, (b) electromagnetic torque and stator current component isy , (c) estimated rotor flux vector module and stator current component isx , (d) stator current components isα,β ; (simulation results), (ωm ref = 0.5 ωmN, tL = 0.75 tN, Rr = var, Rs = var).

6.2. Operation of the PQ-MRAS in Closed-Loop Mode

During further tests, the estimator was operating in the closed-loop mode. Both estimated parameters tracked their real values (Figure 12).The estimated value of the rotor resistance was injected into the control system (to the rotor flux estimator—to the current model) at t = 12 s. It resulted in the elimination of the flux error estimation and the decoupling of the control paths (Figure 13).

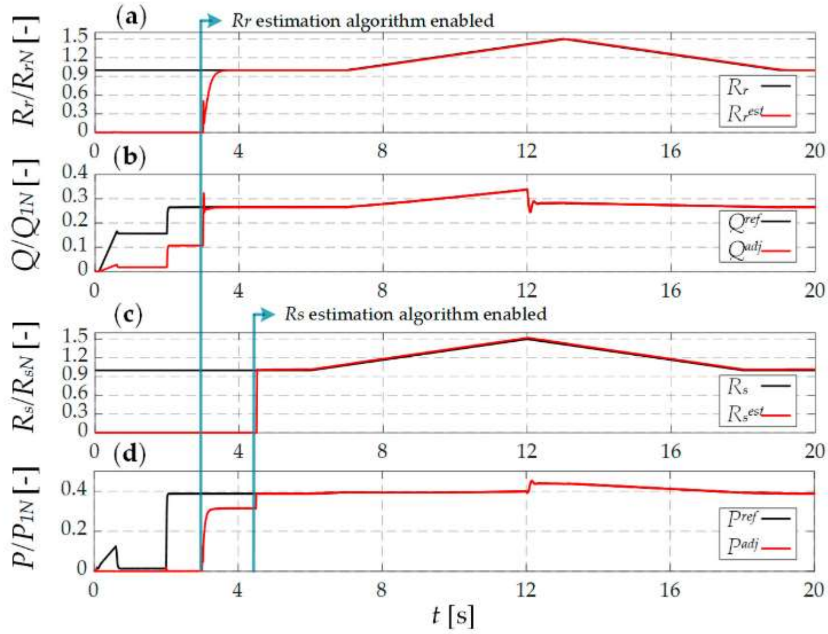

Figure 12. Operation of the PQ-MRAS estimator: (a) estimated rotor resistance, (b) reference and estimated reactive power, (c) estimated stator resistance, (d) reference and estimated active power; (simulation results), (ωm ref = 0.5 ωmN, tL = 0.75 tN, Rr = var, Rs = var).

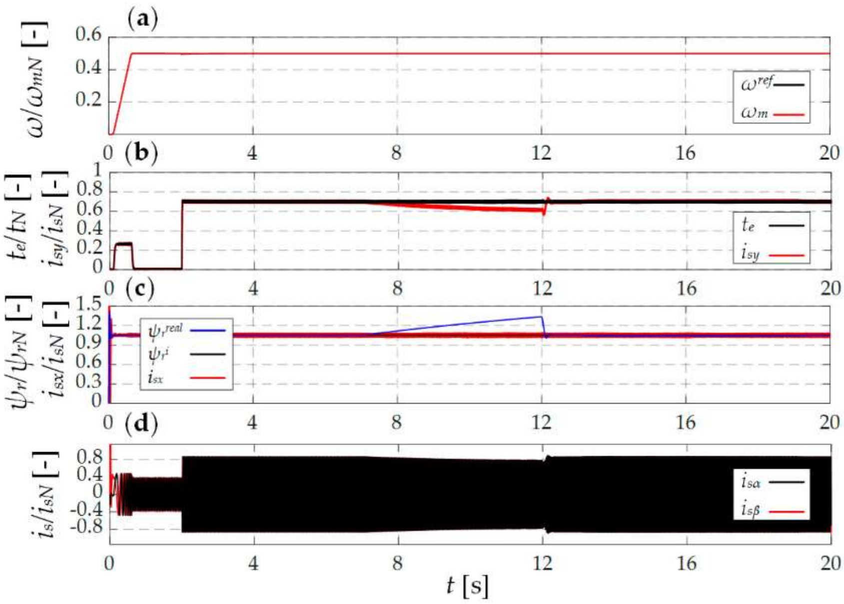

Figure 13. State variables of the drive: (a) reference and measured rotational speed, (b) electromagnetic torque and stator current component isy , (c) estimated rotor flux vector module and stator current component isx , (d) stator current components isα,β ; (simulation results), (ωm ref = 0.5 ωmN, tL = 0.75 tN, Rr = var, Rs = var).

A similar study was performed with a voltage model [1] instead of the current model as the estimator of the rotor flux (18). This estimator directly depends on the stator resistance value (current model depends on rotor resistance). Therefore, it can be used to evaluate P-MRAS operation in the closed-loop mode. The estimated stator resistance was injected into the control system at t = 11 s, which resulted in the improvement of the rotor flux estimation accuracy (Figures 14 and 15).

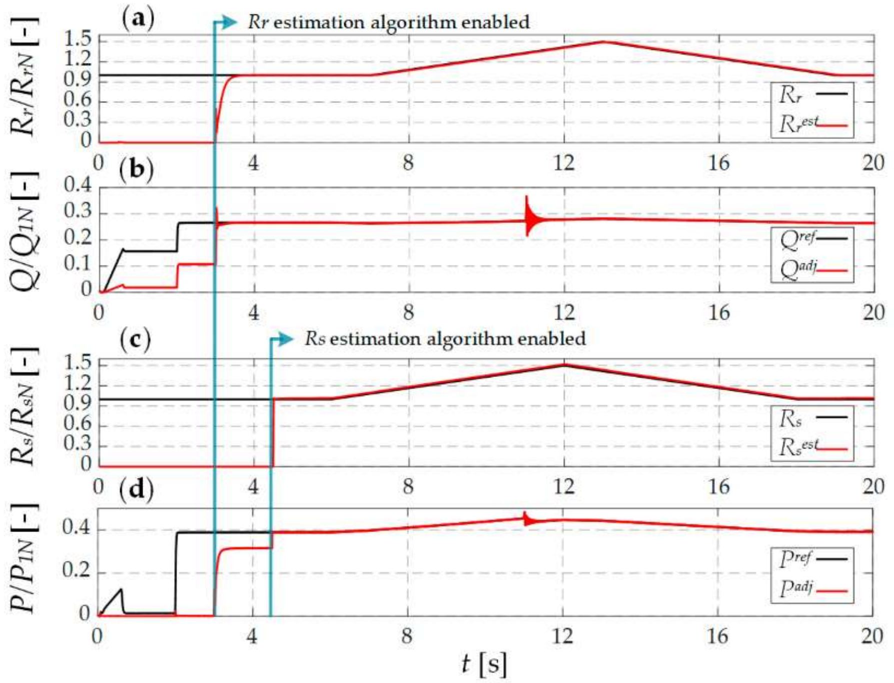

Figure 14. Operation of the PQ-MRAS estimator: (a) estimated rotor resistance, (b) reference and estimated reactive power, (c) estimated stator resistance, (d) reference and estimated active power; (simulation results), (ωm ref = 0.5 ωmN, tL = 0.75 tN, Rr = var, Rs = var).

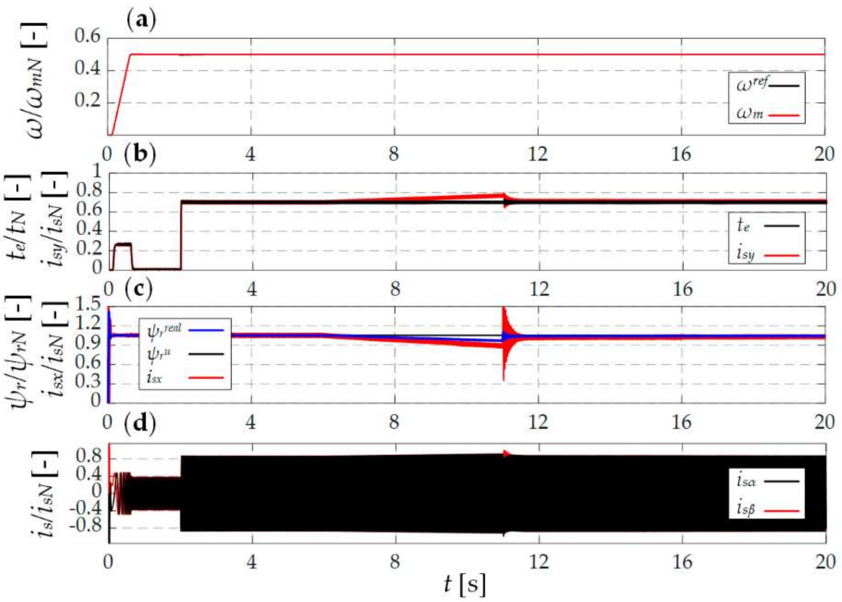

Figure 15. State variables of the drive: (a) reference and measured rotational speed, (b) electromagnetic torque and stator current component isy , (c) estimated rotor flux vector module and stator current component isx , (d) stator current components isα,β ; (simulation results), (ωm ref = 0.5 ωmN, tL = 0.75 tN, Rr = var, Rs = var).

6.3. Rotors' windings faults

At first, the rotor fault detection system was verified. A total rupture of rotor bars was modelled (moments of bars cracking, and their amounts are marked on figures as arrows). Fig. 6 shows the transients of the rotor resistance value and signals from the fault detector.

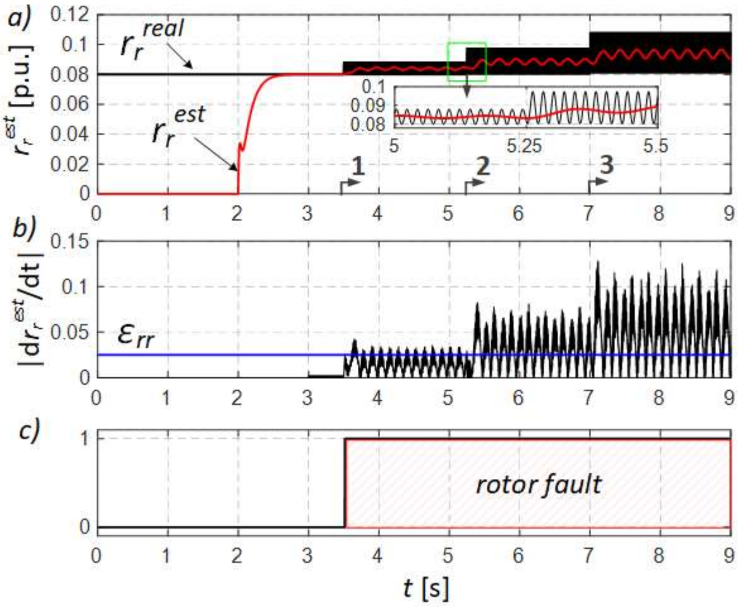

Fig. 6. Rotor winding resistance (a) and detector's signals (b, c) during ruptures of rotor bars; simulation results

It can be observed, that the estimated rotor resistance (R_r) increases according to rotor bars ruptures (Fig. 6a). Consequently, it results in detector activation (Fig. 6b) because the threshold value ε_{rr} is exceeded by the modulus of rotor resistance derivative. Ripples in the rotor resistance transient can be observed as well, what is also visible in the detector derivative signal. Fig. 7 presents the transients of the stator current α and stator current component in axis y.

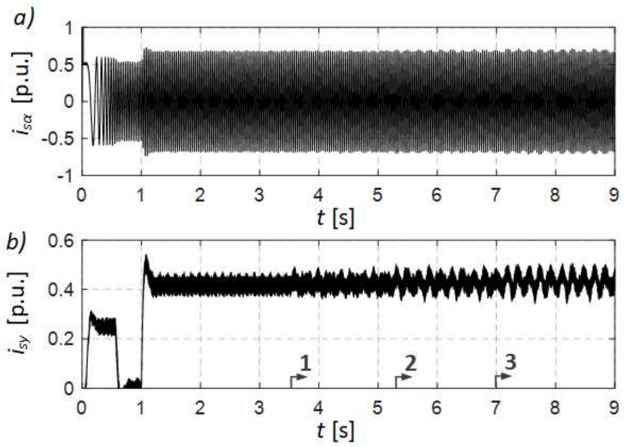

Fig. 7. Stator current components isα (a) and isy (b) during ruptures of rotor bars; simulation results

It is evident that value of the rotor resistance varies as a result of heating (or cooling) process of machines' windings. It may result in incorrect performance of the fault detector. Therefore, other tests were carried out where a linear increase of the rotor resistance was simulated up to 120% of the nominal value. A low slope of the resistance rise was assumed because of fact, that thermal time constant of the machine can reach even several minutes. Results are shown in Fig. 8 – 9.

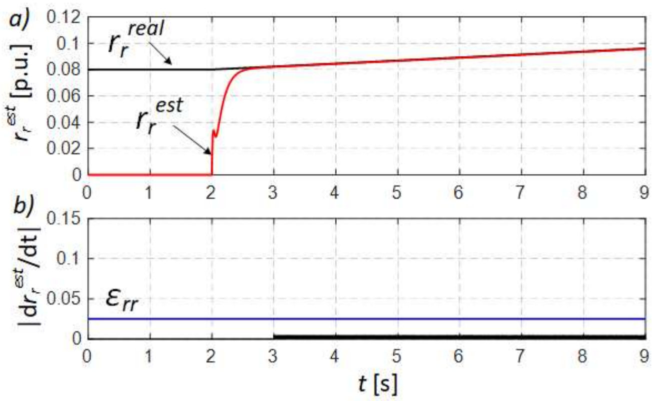

Fig. 8. Rotor winding resistances (a) and detector's signal (b) during heating process; simulation results

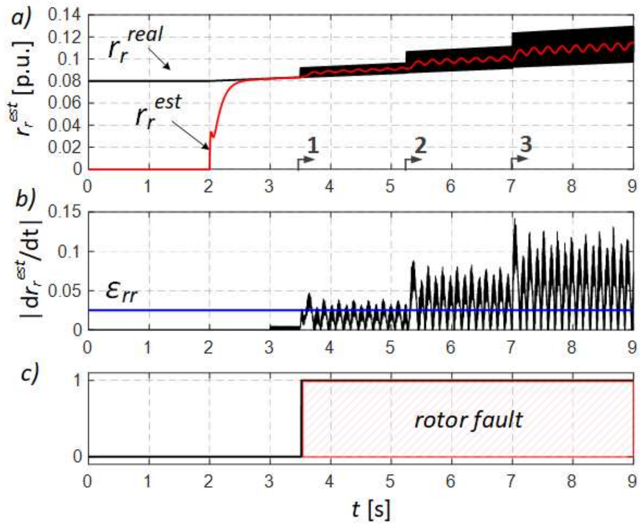

Fig. 9. Rotor winding resistances (a) and detector's signals (b, c) during simultaneous rotors' bars ruptures and heating process; simulation results

It can be noticed, that the derivative value doesn't exceed assumed threshold – variation of rotor resistance due to thermal effects is much slower than due to a bar damage. It can be concluded that proposed rotor fault detector is immune to thermal effects occurring in the machine.

6.4. Stators' windings faults

Subsequently, the stator fault detection system was verified. An ITSC in phase A of stator windings were simulated (moments of turns short and their amounts are marked on figures as arrows). Fig. 10 and Fig. 11 shows transients of the estimated stator resistance, signals from fault detector and stator current components.

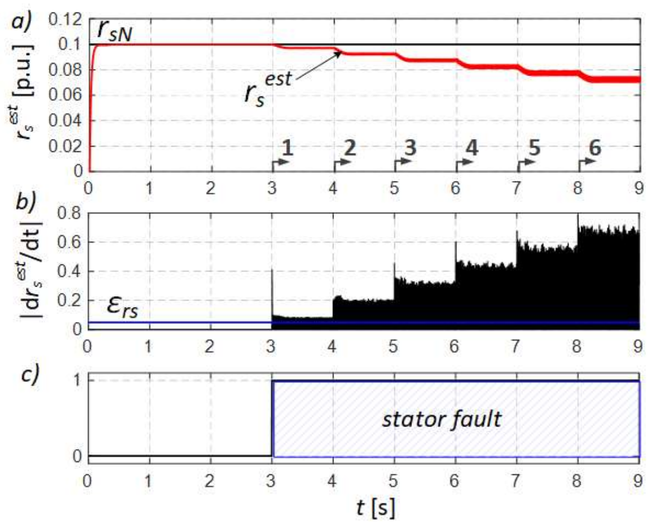

Fig. 10. Stator winding resistance (a) and detector's signals (b, c) during ITCS in phase A; simulation results

It can be observed, that the estimated stator resistance sharply decreases according to short circuits (Fig. 10a). Consequently, it results in the stator's fault detector activation (Fig. 10c) because the threshold value ε_{rs} is exceeded by the modulus of estimated resistance derivative.

The stator current increases due to ITCS and the amplitude level depends on the fault severity (Fig. 11).

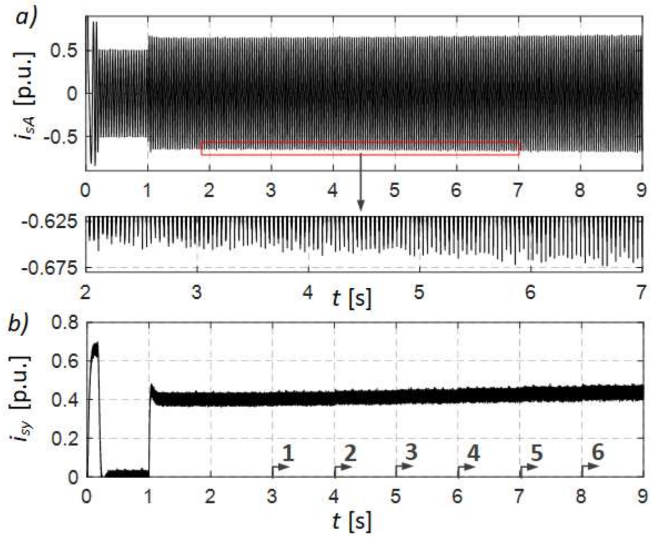

Fig. 11. Stator current in phase A (a) and isy current component (b) during ITSC in phase A; simulation results

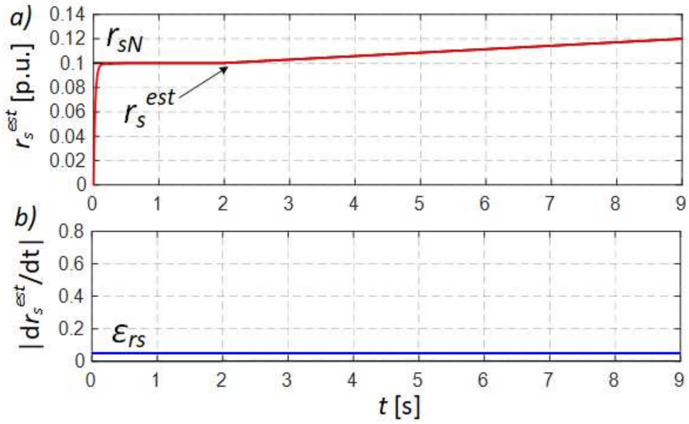

Fig. 12. Stator winding resistance (a) and detector's signal (b) during simultaneous ITSC in phase A and heating process; simulation results

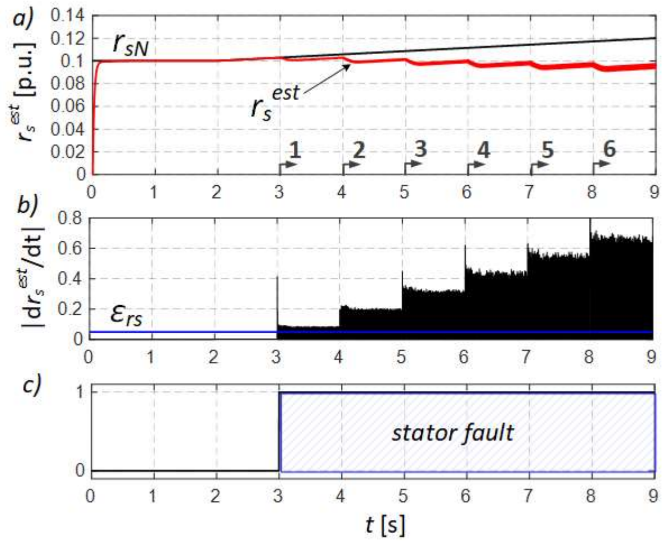

Fig. 13. Stator winding resistance (a) and detector's signals (b, c) during simultaneous ITSC in phase A and heating process; simulation results

Similarly, to the rotor, a value of the stator resistance varies due to heating (or cooling) process of machines' windings. It can provoke incorrect performance of the fault detector as well. Therefore, other tests were performed which were analogous to the case of the rotor faults (a linear increase of the stator resistance were simulated up to 120% of the nominal value). In Fig. 12 it can be noticed, that derivative value doesn't exceed assumed threshold. It can be concluded, that proposed stator fault detector is also immune to thermal effects which are occurred in the machine.

Abbreviations and Symbols

MRAS	Model Reference Adaptive System
IM	Induction Motor
DFOC	Direct Field Oriented Control
DTC	Direct Torque Control
VSI	Voltage Source Inverter
P	Active Power
Q	Reactive Power
u_s	Stator Voltage Vector
i_s	Stator Current Vector
i_r	Rotor Current Vector
ψ_s	Stator Electromagnetic Flux Vector
ψ_r	Rotor Electromagnetic Flux Vector
ω_m	Rotational Shaft Speed
t_e	Electromagnetic Torque
t_l	Load Torque
R_s	Stator Resistance
R_r	Rotor Resistance
L_s	Stator Inductance
L_r	Rotor Inductance
L_m	Magnetizing Inductance
p_b	Number of Pole Pairs
J	Shaft Inertia
ε_P	Estimation Error of the Active Power
ε_Q	Estimation Error of the Reactive Power
K_{PRs}	Coefficient of the Proportional Term in the Stator Resistance Adaptation Mechanism
K_{IRs}	Coefficient of the Integral Term in the Stator Resistance Adaptation Mechanism
K_{PRr}	Coefficient of the Proportional Term in the Rotor Resistance Adaptation Mechanism
K_{IRr}	Coefficient of the Integral Term in the Rotor Resistance Adaptation Mechanism

VII. CONCLUSIONS

In the paper two systems for IM fault detection were proposed. The first one for the rotor's bars cracking detection and the second one for ITSC detection in stator windings. Both systems rely on the hypothesis that each of windings faults results in a sharp change of internal parameters' values of the motor, thus observation and analysis of changes these parameters in a enable to faults detection. Therefore, estimators of IM parameters based on PQ MRAS technique are used to calculate rotor and stator resistances. Obtained resistances are utilized in simple detection algorithms which are based on derivative calculation.

The main feature of both systems is quite simplicity in implementation because they utilized a well-know mathematical model of the IM [2]and derivative algorithm. Moreover, to enable proper operation of the vector control method an on-line identification of the machine's parameters should be applied, nevertheless. On the other hand, PQ MRAS estimators are dependent not only on calculated parameter what is the main problem, but It can be solved by methods mentioned in the paper.

REFERENCES

[1] Bose BK. Power electronics and motor drives: advances and trends. Elsevier; 2006.

[2] Campos-Delgado DU, Espinoza-Trejo DR, Palacios E. Fault-tolerant control in variable speed drives: a survey. IET Electric Power Applications. 2008; 2(2): 121–134.

[3] Riera-Guasp M, Antonino-Daviu JA, Capolino GA. Advances in Electrical Machine, Power Electronic, and Drive Condition Monitoring and Fault Detection: State of the Art. IEEE Transactions on Industrial Electronics. 2015; 62(3): 1746–1759.

[4] Bellini A, Filippetti F, Tassoni C, Capolino GA. Advances in Diagnostic Techniques for Induction Machines. IEEE Transactions on Industrial Electronics. 2008; 55(12): 4109–4126.

[5] Zhang P, Du Y, Habetler TG, Lu B. A Survey of Condition Monitoring and Protection Methods for Medium-Voltage Induction Motors. IEEE Transactions on Industry Applications. 2010; 47(1): 34–46.

[6] Gandhi A, Corrigan T, Parsa L. Recent Advances in Modeling and Online Detection of Stator Interturn Faults in Electrical Motors. IEEE Transactions on Industrial Electronics. 2010; 58(5): 1564–1575.

[7] Siddique A, Yadava GS, Singh B. A review of stator fault monitoring techniques of induction motors. IEEE Transactions on Energy Conversion. 2005; 20(1):106–14.

[8] Ewert P. Application of neural networks and axial flus for the stator and rotor fault detection of induction motor. Power Electronics and Drives. 2018;1–13.

[9] Bellini A, Filippetti F, Franceschini G, Tassoni C. Closed-loop control impact on the diagnosis of induction motors faults. IEEE Transactions on Industry Applications. 2000; 36(5):1318–29.

[10] Cheng S, Zhang P, Habetler TG. An impedance identification approach to sensitive detection and location of stator turn-to-turn faults in a closed-loop multiple-motor drive. IEEE Transactions on Industrial Electronics. 2011; 58(5) : 1545–54.

[11] Tallam RM, Habetler TG, Harley RG. Stator winding turn-fault detection for closed-loop induction motor drives. IEEE Transactions on Industry Applications. 2003; 39(3):1553–7.

[12] Cruz SMA, Cardoso AJM. Diagnosis of Stator Inter-Turn Short Circuits in DTC Induction Motor Drives. IEEE Transactions on Industry Applications. 2004; 40(5):1349–60.

[13] Cruz SMA, Cardoso AJM. Fault Indicators for the Diagnosis of Rotor Faults in FOC Induction Motor Drives. In: 2007 IEEE International Electric Machines & Drives Conference; 1136–41.

[14] Wolkiewicz M, Tarchała G, Orłowska-Kowalska T, Kowalski CT. Online Stator Interturn Short Circuits Monitoring in the DFOC Induction-Motor Drive. IEEE Transactions on Industrial Electronics. 2016;63(4):2517–28.

[15] Wolkiewicz M, Tarchała G, Kowalski T, Orłowska-Kowalska T. Advanced Control of Electrical Drives and Power Electronic Converters. 2017; 75:169-191.

[16] Wolkiewicz M, Tarchała G, Orłowska-Kowalska T. Diagnosis of stator and rotor faults of an induction motor in closed-loop control structure. In: 2018 International Symposium on Power Electronics, Electrical Drives, Automation and Motion (SPEEDAM); 2018. 196–201.

[17] Iserman R. Fault-Diagnosis Applications, Model-Based Condition Monitoring: Actuators, Drives, Machinery, Plants, Sensors, and Fault-tolerant Systems. Springer-Verlag Berlin Heidelberg; 2011.

[18] Gao Z, Cecati C, Ding SX. A Survey of Fault Diagnosis and Fault-Tolerant Techniques—Part I: Fault Diagnosis with Model-Based and Signal-Based Approaches. IEEE Transactions on Industrial Electronics. 2015; 62(6):3757–67.

[19] Cho KR, Lang JH, Umans SD. Detection of broken rotor bars in induction motors using state and parameter estimation. IEEE Transactions on Industry Applications.1992;28(3):702–709.

[20] Bachir S, Tnani S, Trigeassou JC, Champenois G. Diagnosis by parameter estimation of stator and rotor faults occurring in induction machines. IEEE Transactions on Industrial Electronics. 2006; 53(3):963–73.

[21] Said MSN, Benbouzid MEH, Benchaib A. Detection of broken bars in induction motors using an extended Kalman filter for rotor resistance sensorless estimation. IEEE Transactions on Energy Conversion. 2000;15(1):66–70.

[22] Bachir S, Trigeassou JC, Tnani S. On-Line Stator Faults Diagnosis By Parameter Estimation. In: European Conference on Power Electronics and Applications (EPE); 2003. p. 209–19.

[23] Kowalski CT, Wierzbicki R, Wolkiewicz M. Stator and Rotor Faults Monitoring of the Inverter-Fed Induction Motor Drive using State Estimators. Automatika. 2013;54(3):348–55.

[24] Bazine IBA, Tnani S, Poinot T, Champenois G, Jelassi K. On-line detection of stator and rotor faults occurring in induction machine diagnosis by parameters estimation. In: 8th IEEE Symposium on Diagnostics for Electrical Machines, Power Electronics & Drives; 2011: 105–12.

[25] Karami F, Poshtan J, Poshtan M. Detection of broken rotor bars in induction motors using nonlinear

Kalman filters. ISA Transactions. 2010;49(2):189–95.

[26] Nguyen V, Wang D, Seshadrinath J, Nadarajan S, Vaiyapuri V. Fault severity estimation using nonlinear Kalman filter for induction motors under inter-turn fault. In: 42nd Annual Conference of the IEEE Industrial Electronics Society (IECON); 2016: 1488–93.

[27] Nguyen V, Wang D, Seshadrinath J, Ukil A, Krishna MS, Nadarajan S. A Method for Incipient Interturn Fault Detection and Severity Estimation of Induction Motors Under Inherent Asymmetry and Voltage Imbalance. IEEE Transactions on Transportation Electrification. 2017;3(3):703–15.

[28] Kallesøe CS, Izadi-Zamanabadi R, Vadstrup PP, Rasmussen H. Observer-based estimation of stator-winding faults in delta-connected induction motors: A linear matrix inequality approach. IEEE Transactions on Industry Applications. 2007;43(4):1022–31

[29] De Angelo CH, Bossio GR, Giaccone SJ, Valla MI, Solsona JA, Garcia GO. Online Model-Based Stator-Fault Detection and Identification in Induction Motors. IEEE Transactions on Industrial Electronics. 2009;56(11):4671–80.

[30] Abdallah H, Benatman K. Stator winding inter-turn short-circuit detection in induction motors by parameter identification. IET Electric Power Applications. 2017;11(2):272–88.

[31] Chouiref H, Boussaid B, Abdelkrim MN, Aubrun C. Nonlinear fault tolerant control-based parameter estimation diagnosis: Application to induction motors. In: 10th International Multi-Conferences on Systems, Signals & Devices (SSD); 2013:1–6.

[32] Treetrong J. Electric Motor Fault Diagnosis Based on Parameter Estimation Approach Using Genetic Algorithm. In: International Multi Conference of Engineers and Computer Scientist (IMECS); 2010.

[33] Duan F, Zivanovic R. Condition Monitoring of an Induction Motor Stator Windings Via Global Optimization Based on the Hyperbolic Cross Points. IEEE Transactions on Industrial Electronics. 2015;62(3):1826–34.

[34] Sellami T, Berriri H, Jelassi S, Mimouni MF. Sliding mode observer-based fault-detection of inter-turn short-circuit in induction motor. In: 14th International Conference on Sciences and Techniques of Automatic Control & Computer Engineering - STA'2013; 2013:524–529.

[35] Toliyat HA, Levi E, Raina M. A review of RFO induction motor parameter estimation techniques. IEEE Transactions on Energy Conversion. 2003;18(2):271–83.

[36] Syam P, Kumar R, Das S, Chattopadhyay AK. Review on model reference adaptive system for sensorless vector control of induction motor drives. IET Electric Power Applications. 2015;9(7):496–511.

[37] Zorgani Y, Jouili M, Koubaa Y. A very low speed sensorless control induction motor drive with online rotor resistance using MRAS Scheme. Power Electronics and Drives. 2018; 3(38) : 171–186.

[38] Zorgani YA, Koubaa Y, Boussak M. Sensorless speed control with MRAS for induction motor drive. In: XXth International Conference on Electrical Machines (ICEM); 2012:2259 – 65.

[39] Bednarz SA, Dybkowski M. On-line detection of the rotor faults in the induction motor drive using parameter estimator. In: 2018 International Symposium on Electrical Machines (SME); 2018. p. 1–5.

[40] Vasic V, Vukosavic SN, Levi E. A stator resistance estimation scheme for speed sensorless rotor flux-oriented induction motor drives. IEEE Trans Energy Convers. 2003 Dec;18(4) : 476–83.

[41] Bednarz SA, Dybkowski M, Wolkiewicz M., Identification of the Stator Faults in the Induction Motor Drives Using Parameter Estimator. In: IEEE 18th International Power Electronics and Motion Control Conference (PEMC); 2018. p. 688–93.

[42] Pawlak M, Orłowska-Kowalska T. Application of the simplified two axial model for rotor faults modeling of the induction motor. Przegląd Elektrotechniczny. 2006;82(10):48–53. Polish.

[43] Kaźmierkowski MP, Krishnan R, Blaabjerg F. Control in power electronics: selected problems. Elsevier; 2003.

[44] Dybkowski M. Universal Speed and Flux Estimator for Induction Motor. Power Electron Drives. 2018;3(1):157–69.

[45] Dybkowski, M.; Bednarz, S.A. Simultaneous Estimation of the Stator and Rotor Resistances in an Induction Motor Drive using Novel Active and Reactive Power Based Model Reference Adaptive System. In Proceedings of the 2019 International Conference on Electrical Drives and Power Electronics (EDPE), The High Tatras, Slovakia, 24–26 September 2019.

[46] Perng, S.; Lai, Y.; Liu, C. Sensorless vector controller for induction motor drives with parameter identification. In Proceedings of the 24th Annual Conference of the IEEE Industrial Electronics

Society (IECON), Aachen, Germany, 31 August–4 September 1998.
[47] Madadi Kojabadi, H.; Abarzadeh, M.; Aghaei Farouji, S. Robust stator resistance identification of an IM drive using model reference adaptive system. Energy Convers. Manag. **2013**, 65, 507–517.
[48] Mapelli, F.L.; Tarsitano, D.; Cheli, F. A rotor resistance MRAS estimator for EV induction motor traction drive based on torque and reactive stator power: Simulation and experimental results. In Proceedings of the 2014 International Conference on Electrical Machines (ICEM), Berlin, Germany, 2–5 September 2014.
[49] Holtz, J. Sensorless Control of Induction Motor Drives. Proc. IEEE **2002**, 90, 1359–1394.
[50] Kazmierkowski, M.P.; Krishann, F.; Blabjerg, F. Control in Power Electronics: Selected Problems, 1st ed.; Academic Press: San Diego, CA, USA, 2002.